The Eurasia Proceedings of Science, Technology, Engineering & Mathematics (EPSTEM)
ISSN: 2602-3199

The Eurasia Proceedings of Science, Technology, Engineering & Mathematics (EPSTEM), 2024

Volume 29, Pages 128-144

ICRETS 2024: International Conference on Research in Engineering, Technology and Science

Shear Force in RC Internal Beam-Column Connections for a Beam Loaded With a Transverse Force Occupying Different Possible Positions

Albena Doicheva
University of Architecture, Civil Engineering and Geodesy (UACEG)

Abstract: Frame structures are vulnerable to seismic impacts. The frame joint is the element that is often responsible for compromising frame structures. In recent years, shear force in the beam-column connection has been pointed out as the main culprit for damage in the nodes, and from there to the entire structure. The complex nature of the stressed and strained state of the joint is due to the poor knowledge of the forces passing in the beam-beam or column-column direction. For their more accurate determination, one departs from the standard acceptance of the static scheme of the axis line of the structural elements and works with their actual dimensions. With a skillful selection of the support devices, a mathematical model of the beam is created, allowing the determination of the forces that arise along its height and that enter the joint. The magnitudes of the support reactions of the beam are applicable both to operation in the elastic stage and to the plasticization of the beam and the occurrence of a crack between the beam and the column on the face of the column. In the present work, a cantilever beam loaded with a transverse force, occupying different possible positions on the beam, is considered. The expressions for the support reactions are derived. The unfavorable position of the loading force, which results in the greatest shear force, was investigated. A comparison is made of the corresponding shear force in the beam-to-column connection, with that recommended in the literature. The results demonstrate differences of up to 18.20%. The main parameters of the cantilever beam that were monitored are cross-sectional shape, modulus of elasticity of concrete and position of the loading force.

Keywords: Beam-to-column connection, Shear force, Reinforced concrete, Large deformations, Cracking in the beam

Introduction

One of the main elements in frame structures is the beam-column connection. Its main task is to ensure the not hindered passage of forces in the beam-beam and column-column direction while preserving the integrity of the beam-column connection. Disturbances in the beam-column joint are often responsible for the damage of part of the buildings or even their destruction. Over the past few decades, many frame structures have experienced sudden failure due to joint shear during cyclic loading, such as earthquakes.

The first quantitative definition of shear strength was given in Hanson and Connor (1967). In their report on the test results of RC interior beam-column connections, the researchers defined joint shear as the horizontal force transferred to the mid-horizontal plane in a beam-column connection. They suggest that joint shear failure can be prevented by limiting the joint shear stress to the level at which joint shear failure occurs.

Based on the assumption made, design codes of different countries are created. They provided a limit value of the shear stress of the joint. Detailed review of interior and exterior joints of special moment resisting reinforced concrete frames, with reference to three codes of practices: American Concrete Institute (ACI 318M-02), New Zealand Standards (NZS 3101:1995) and Eurocode 8 (EN 1998-1 :2003) was performed by Uma & Sudhir, (2006). A number of parameters have been defined that affect the shear strength of the joint. Researchers from different countries rely on different combinations of parameters (Park & Paulay, 1975; Paulay, 1989; Lowes &

- Selection and peer-review under responsibility of the Organizing Committee of the Conference

Altoontash, 2003; Celik & Ellingwood, 2008; Tran et al., 2014; Gombosuren & Maki, 2020). This makes it impossible to create a worldwide uniform procedure for designing the shear force in the beam-column connection.

In Bakir and Boduroglu (2001), parametric studies were carried out on various parameters influencing the shear strength of the joint. The results of multiple studies on 5 parameters in relation to different countries are summarized. One of the main conclusions that emerge is that "the strength of the concrete cylinder increases the shear strength of the joint".

In Yuan et al., 2013, “a number of RC/ECC composite beam-column joints have been tested under reversed cyclic loading to study the effect of substitution of concrete with ECC in the joint zone on the seismic behaviors of composite members.” “The substitution of concrete with ECC in the joint zone was experimentally proved to be an effective method to increase the seismic resistance of beam-column joint specimens.”

In Doicheva et al. (2023-3) Seismic tests on reinforced concrete beam-column joint sub-assemblages subject to lateral and long-term vertical load was reported. The influence of an additional transverse force on the beam applied near the support of the cantilever beam is observed. It was reported that such a force did not significantly affect the beam column connection.

Shiohara (2001) proposed a new model for calculating and detailing the beam-column connection based on the capacitive design. The study shows an irrationality in the joint shear model adopted in the most current codes for the design of reinforced concrete beam-column joints. The conclusions are based on the experimental test data of twenty reinforced concrete internal beam-column connections damaged by joint shear. The analysis showed that the joint shear stress increased in most specimens, even after the initiation of apparent joint shear failure.

Problem

Hanson and Connor (1967) gave the first quantitative definition of the joint shear in an interior beam-column connection from Figure 1. The researchers defined it with Eq. (1). This is an internal force acting on the free body along the horizontal plane at the midheight of the beam-column connection.

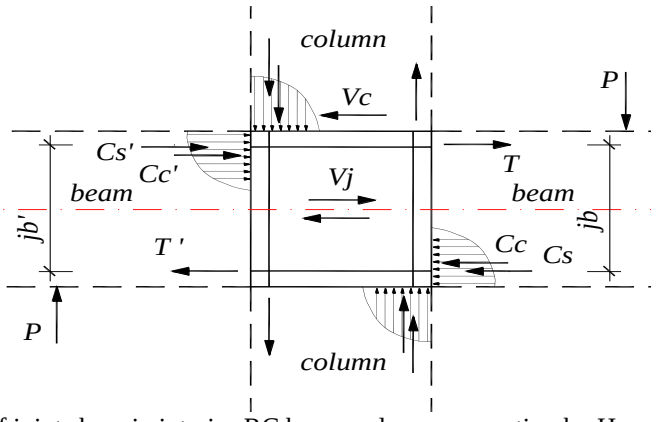

Figure 1. Definition of joint shear in interior RC beam-column connection by Hanson and Connor (1967)

$$V_j = T + C_S' + C_C' - V_C = T + T' - V_C \tag{1}$$

where: C_S and C_S' - compressive force in bottom and top longitudinal reinforcing bars in beam passing through the connection;

C_C and C_C' - compressive force in concrete on the bottom and top edge of beam;

T and T' - tensile forces in top and bottom reinforcing bars in beam passing through the connection;

V_C - column shear force

The contribution of steel and concrete is taken into account separately. This definition is clear and has been used in the design of beam-column connections in different countries.

The difficulty encountered in determining the forces T and T' from Eq. (1) leads to the adoption of another way of writing the expression for the shear force in the literature. Usually T and T' are defined by Eq. (2).

$$T = \frac{M_b}{j_b} \text{ and } T' = \frac{M'_b}{j_b} \tag{2}$$

where: M_b and M'_b - moment at column face;

j_b and j'_b - the length of bending moment arm at the column face. It is assumed to be constant and unchanging in the process of deformation.

Then Eq. (1) is rewritten from moment in the beam section at column faces into Eq. (3).

$$V_j = \frac{M_b}{j_b} + \frac{M'_b}{j'_b} - V_C \tag{3}$$

The assumption (2) obliges us to assume equal forces in the bottom and top reinforcement of the beam at the face of the column. In the author's previous publications, these values were shown to differ substantially (Doicheva, 2021), (Doicheva, 2022), (Doicheva, 2023-1), (Doicheva, 2023-2).

In this article, the following tasks are set: 1. to determine expressions for the forces from Figure 1, at the column face for a cantilever beam loaded with a transverse force, occupying different possible positions on the beam. 2. to perform comparisons of the obtained results with the results of Eq. (2) and Eq. (3).

Method

Mathematical Model of Beams

A cantilever beam is considered. The beam is statically indeterminate and prismatic. The beam is under the conditions of special bending with tension/compretion and Bernoulli-Euler hypothesis is considered.

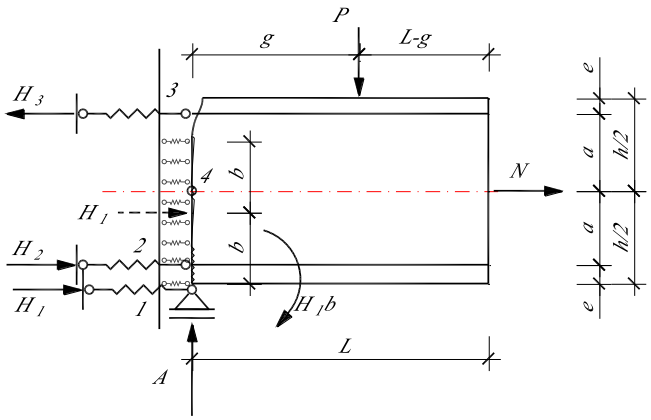

Figure 2. Supports of cantilever beam to column and symmetrical cross section

The beam is loaded with a vertical force $P\,[kN]$, which changes its position on the beam. It is monitored by the distance $g\,[cm]$. The support takes place in vertical support 1, where a vertical support reaction occurs $A\,[kN]$. At the level of the reinforcing bars, elastic supports 2 and 3, with linear spring coefficients k_2 and k_3, are introduced. They are set as the reduced tension/compression stiffness of the reinforcing bar, Eq. (4).

$$k_2 = \frac{E_2 A_2}{L} \quad \text{and} \quad k_3 = \frac{E_3 A_3}{L} \tag{4}$$

where: $L\,[cm]$ - the length of the beam;

$A_2\left[cm^2\right]$ and $A_3\left[cm^2\right]$ - the area of the cross-section of bottom and top longitudinal reinforcing bars in beam passing through the connection;

$E_2\left[kN/cm^2\right]$ and $E_3\left[kN/cm^2\right]$ - the modulus of elasticity of the bottom and top longitudinal reinforcing bars in beam passing through the connection

The supporting reactions that occur here are $H_2\left[kN\right]$ and $H_3\left[kN\right]$.

Linear spring supports act along the vertical edge of the beam, taking into account the connection of the concrete of the beam with that of the column. The forces in all the springs are reduced to one force, $H_1\left[kN\right]$. In case of large deformations, part of the vertical edge is destroyed. The unbroken edge has length $2b\left[cm\right]$. The reaction $H_1\left[kN\right]$, which is symmetrically located with respect to the intact lateral edge, moves along the height of the beam as the crack length increases. For convenience, it has been transferred $H_1\left[kN\right]$ to the support along the bottom edge (support one), after applying Poinsot's theorem concerning the transfer of forces in parallel to their directrix. This necessitated the introduction of compensating moments $H_1 b\left[kN.cm\right]$. The coefficient of the linear spring is k_1. It is set as the reduced tensile/compressive stiffness of the concrete section, Eq. (5).

$$k_1 = \frac{E_1 A_1}{L} \tag{5}$$

where: $L\left[cm\right]$ - the length of the beam;

$A_1\left[cm^2\right]$ - the area of the cross-section of the concrete

$E_1\left[kN/cm^2\right]$ - the modulus of elasticity of the concrete

As a consequence of the linear deformations in the cantilever beam, a normal axial force occurs $N\left[kN\right]$, which is introduced at the free end.

Symmetric Cross-Section

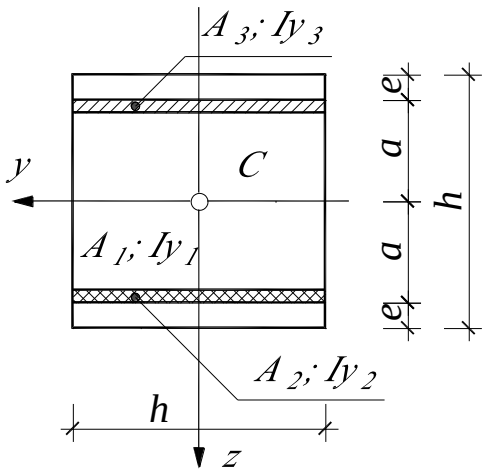

Figure 3. Symmetrical cross-section of the beam

The following notations have also been introduced:

$h\left[cm\right]$ - the heigth of the beam;

$e\left[cm\right]$ and $a\left[cm\right]$ - offset of the reinforcing bars from the top and bottom edges of the beam and from the axis of the beam, respectively;

$EA = E_1A_1 + E_2A_2 + E_3A_3$ - tensile (compressive) stiffness of the composite section, where E_2A_2, E_3A_3 and E_1A_1 are tensile (compressive) stiffness of the reinforcing bars and of the concrete, respectively;

$EI = E_1I_1 + E_2I_2 + E_3I_3$ - bending stiffness of the composite section, where E_2I_2, E_3I_3 and E_1I_1 are bending stiffness of the reinforcing bars and of the concrete cross-section, respectively;

$I_1\left(I_{y1}\right)$, $I_2\left(I_{y2}\right)$ and $I_3\left(I_{y3}\right)$ are the moment of inertia of the concrete cross-section and of the top and bottom reinforcing bars relative to the principal axis of inertia *y*.

Support Reactions

The three equilibrium conditions of statics give us respectively:

$$1.\sum V = 0 \quad \rightarrow \quad A = P \tag{6}$$

$$2.\sum H = 0 \quad \rightarrow \quad N = H_3 - H_1 - H_2 \tag{7}$$

$$3.\sum M_4 = 0 \quad \rightarrow \quad -Pg - H_1b + H_3a + H_2a + H_1\frac{h}{2} = 0 \tag{8}$$

From Eq. (8) we express H_2:

$$H_2 = \frac{Pg - H_1\left(\frac{h}{2} - b\right)}{a} - H_3 \tag{9}$$

The solution is based on Menabria's theorem about statically indeterminate systems in first-order theory.

The potential energy of deformation in special bending, combined with tension (compressure) and with the effect of linear springs taken into account, will be, Eq. (10):

$$\Pi = \frac{1}{2}\int_0^L \frac{M^2(x)}{EI}dx + \frac{1}{2}\int_0^L \frac{N^2(x)}{EA}dx + \frac{H_1^2}{2k_1} + \frac{H_2^2}{2k_2} + \frac{H_3^2}{2k_3}. \tag{10}$$

It is a well-known fact that, according to Menabria's theorem, the desired hyperstatic unknown is determined by the minimum potential energy condition with respect to it or will be, Eq. (11):

$$\frac{\partial\Pi}{\partial H_1} = 0; \quad \frac{\partial\Pi}{\partial H_2} = 0; \quad \frac{\partial\Pi}{\partial H_3} = 0. \tag{11}$$

The beam is twice statically indeterminate. This leads to using the first and third terms of Eq. (11).

The bending moments for the two parts of beam are:

$$M_1(x) = Ax + H_1b - H_1\frac{h}{2} - H_2a - H_3a, \tag{12}$$

$$M_2(x) = A(g + x) + H_1b - H_1\frac{h}{2} - H_2a - H_3a - Pg, \tag{13}$$

Substitute Eq. (6) in Eq. (12) and Eq. (13). Substitute the resulting expressions and Eq. (9), together with Eq. (7) in Eq. (10). We perform operations from Eq. (11). A system of two linear equations with respect to the two unknowns, $H_1; H_3$, is obtained. Substitute the obtained $H_1; H_3$ in Eq. (9), to express H_2. The solutions give the formulas of the three horizontal support reactions below:

$$H_1 = \frac{-Pgk_1\left\{EAh_1R_1 + 2EIL\left[k_2 2a - k_3n_2\right] + 2Lga^2K_{23}n_2\right\}}{EI\left\{EAD_1 + D_2\right\}} \tag{14}$$

$$H_2 = \frac{Pgk_2\left\{EAaR_2 + 8EILa\left[k_1 + k_3\right] + LgaK_{13}n_2^2\right\}}{2EI\left\{EAD_1 + D_2\right\}} \tag{15}$$

$$H_3 = \frac{Pgk_3\left\{4EAaR_1 + 4EIL\left[k_1n_2 + k_2 2a\right] - LgaK_{12}n_1n_2\right\}}{2EI\left\{EAD_1 + D_2\right\}} \tag{16}$$

where $h_1 = 2b - h$; $n_1 = 2a + h_1$; $n_2 = 2a - h_1$;

$K_{12} = k_1k_2$; $K_{13} = k_1k_3$; $K_{23} = k_2k_3$;

$R_1 = 2EI - k_2ga^2$; $R_2 = 8EI + g\left(k_1h_1^2 + k_3 4a^2\right)$;

$D_1 = \left(k_2 + k_3\right)4a^2 + k_1h_1^2$; $D_2 = L\left[2ak_1k_2n_1 + k_1k_3n_2^2 + k_2k_3 8a^2\right]$ (17)

The positions of the force *P*, for which the support reactions H_1, H_2 and H_3 have an extremum with respect to the distance g, are respectively:

$$g_{H_1} = \frac{EA2EI\left\{h_1 + L\left[k_2 2a - k_3n_2\right]\right\}}{2\left[EAa^2k_2h_1 - 2La^2K_{23}n_2\right]} \tag{18}$$

$$g_{H_2} = \frac{8EI\left[EA + L\left(k_1 + k_3\right)\right]}{-2\left[EA\left(4a^2k_3 + k_1h_1^2\right)\right] - LK_{13}n_2^2} \tag{19}$$

$$g_{H_3} = \frac{4EI\left\{2EAa + L\left[k_2 2a - k_1n_2\right]\right\}}{2a\left[4EAa^2k_2 + LK_{12}n_1n_2\right]} \tag{20}$$

We perform the same solution without considering the axial force in the potential energy expression. The support reactions are respectively:

$$H_1 = \frac{-Pgk_1h_1R_1}{EI\left[4a^2\left(k_2 + k_3\right) + k_1h_1^2\right]} \tag{21}$$

$$H_2 = \frac{Pagk_2R_2}{2EI\left[4a^2\left(k_2 + k_3\right) + k_1h_1^2\right]} \tag{22}$$

$$H_3 = \frac{2Pagk_3R_1}{EI\left[4a^2\left(k_2 + k_3\right) + k_1h_1^2\right]} \tag{23}$$

The maximum value of the support reactions is obtained when the loading force is located at a distance g from the support, respectively.:

$$g_{H_1} = \frac{EI}{k_2a^2}; \quad g_{H_2} = \frac{-8EI}{-2\left(4a^2k_3 + k_1h_1^2\right)}; \quad g_{H_3} = \frac{EI}{2k_2a^2} \tag{24}$$

Asymmetric Cross-Section

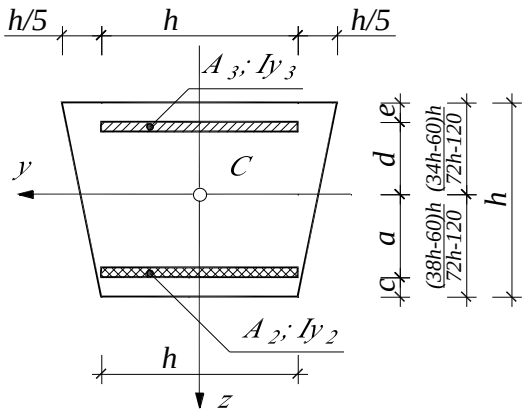

Figure 4. Asymmetrical cross-section of the beam

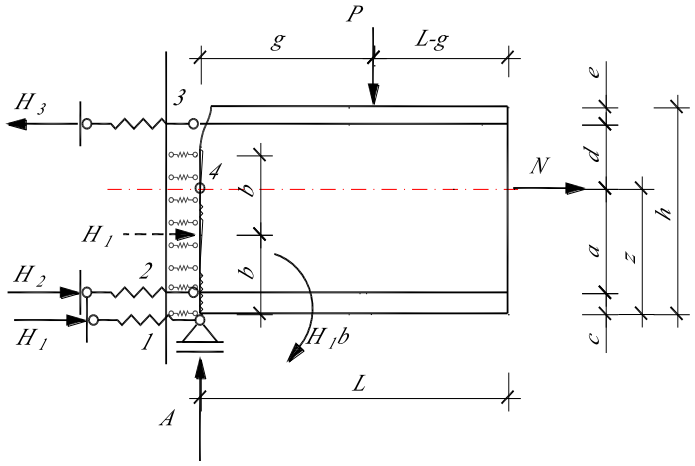

Figure 5. Supports of cantilever beam to column and asymmetrical cross section

The dimensions that are different for the asymmetrical beam compared to the symmetrical one are:

$c[cm]$ and $e[cm]$ - offset of the reinforcing bars from the top and the bottom edges of the beam, respectively;

$a[cm]$ and $d[cm]$ - offset of the top and the bottom reinforcing bars from the axis of the beam, respectively;

$z[cm]$ - offset of the principal axis of inertia *y* to the bottom edge of the beam;

The equilibrium conditions from statics are Eq. (6) and Eq. (7). Then Eq. (8) will be:

$$3.\sum M_4 = 0 \quad \rightarrow \quad -Pg - H_1 b + H_3 d + H_2 a + H_1 z = 0 \tag{25}$$

From Eq. (25) we express H_2:

$$H_2 = \frac{Pg - H_1(z-b) - H_3 d}{a} \tag{26}$$

The bending moments for the two parts of the beam are respectively:

$$M_1(x) = Ax + H_1 b - H_1 z - H_2 a - H_3 d \tag{27}$$

$$M_2(x) = A(g+x) + H_1 b - H_1 z - H_2 a - H_3 d - Pg\,, \tag{28}$$

The solution is performed as described for the symmetric section solution. The three supporting reactions are:

$$H_1 = \frac{-Pgk_1\left\{EAh_2R_1 + 2EIL\left[k_2 a + k_3 n_4\right] - LgaK_{23}(a+d)n_4\right\}}{2EI\left\{EAD_3 + D_4\right\}} \tag{29}$$

$$H_2 = \frac{Pgk_2\left\{EAaR_3 + 2EILa\left[k_1 + k_3\right] + LgaK_{13}n_4^2\right\}}{2EI\left\{EAD_3 + D_4\right\}} \tag{30}$$

$$H_3 = \frac{Pgk_3\left\{EAdR_1 + 2EIL\left[k_2 a - k_1 n_4\right] - LgK_{12}a\left(an_4 + h_2^2 - dh_2\right)\right\}}{2EI\left\{EAD_3 + D_4\right\}} \tag{31}$$

where $h_2 = b - z$; $n_3 = d + h_2$; $n_4 = h_2 - d$;

$K_{12} = k_1 k_2$; $K_{13} = k_1 k_3$; $K_{23} = k_2 k_3$;

$R_1 = 2EI - k_2 g a^2$; $R_3 = 2EI + g\left(k_1 h_2^2 + k_3 d^2\right)$;

$D_3 = k_1 h_2^2 + k_2 a^2 + k_3 d^2$; $D_4 = L\left[ak_1 k_2\left(a + h_2\right) + k_1 k_3 n_4^2 + k_2 k_3 a(a+d)\right]$ (32)

The extremum study of Eq. (29), Eq. (30) and Eq. (31) with respect to the position of the load *P* gives us the expressions for *g* to the three support reactions.

$$g_{H_1} = \frac{EA2EI\left\{h_2 + L\left[k_2 a + k_3 n_4\right]\right\}}{2\left[EAa^2 k_2 h_2 + LaK_{23}\left(a+d\right)n_4\right]} \tag{33}$$

$$g_{H_2} = \frac{2EI\left[EA + L\left(k_1 + k_3\right)\right]}{2\left[-EA\left(d^2 k_3 + k_1 h_2^2\right) - LK_{13}n_4^2\right]} \tag{34}$$

$$g_{H_3} = \frac{2EI\left\{EAd + L\left[k_2 a - k_1 n_4\right]\right\}}{2a\left[EAda^2 k_2 + LK_{12}a\left(an_4 + h_2^2 - dh_2\right)\right]} \tag{35}$$

A solution for an asymmetrical section was performed without considering the axial force in the strain potential energy expression.

$$H_1 = \frac{-Pgk_1 h_2 R_1}{2EI\left[k_2 a^2 + k_3 d^2 + k_1 h_2^2\right]} \tag{36}$$

$$H_2 = \frac{Pagk_2 R_2}{2EI\left[k_2 a^2 + k_3 d^2 + k_1 h_2^2\right]} \tag{37}$$

$$H_3 = \frac{Pdgk_3 R_1}{2EI\left[k_2 a^2 + k_3 d^2 + k_1 h_2^2\right]} \tag{38}$$

The support reactions have an extremum with respect to the distance *g*, which gives the position of the force *P*. For each support reaction, it is respectively:

$$g_{H_1} = \frac{EI}{k_2 a^2}; \quad g_{H_2} = \frac{-2EI}{2\left(k_3 d^2 + k_1 h_2^2\right)}; \quad g_{H_3} = \frac{EI}{k_2 a^2} \tag{39}$$

The all solutions was performed in the symbolic environment of the MATLAB R2017b program.

Results and Discussion

For the numerical results, a beam with a cross-section of $75/75\,cm$ and $30/30\,cm$ were introduced. For all examples considered $P = const$, the distances $e = 3\left[cm\right]$ and $c = 3\left[cm\right]$. And more $A_2 = A_3 = 75\left[cm^2\right]$ for a cross-section of $75/75\,cm$ and $A_2 = A_3 = 30\left[cm^2\right]$ for a cross-section of $30/30\,cm$. The modulus of elasticity of reinforcing bars are $E_2 = E_3 = 39000\left[kN/cm^2\right]$. Two examples with a difference only in the modulus of elasticity of concrete are considered. The modules used are $E_1 = 1700\left[kN/cm^2\right]$ for normal concrete and $E_1 = 3900\left[kN/cm^2\right]$ for High-strength concrete. The beam is with a length of $L = 200\,cm$.

Case I – Symmetrical Cross Section

The distance $b\left[cm\right]$ varies in the interval $\left[37.5, 0\right)$ and $\left[15, 0\right)$ for a cross-section of $75/75\,cm$ and $30/30\,cm$, respectivly. It is monitored by the ratio h/b. In Figure. 6 shows the variation of the parameters of the three support reactions for two cross-sections - *75/75cm* and *30/30cm*, with two modulus of elasticity of the concrete - E_1*=1700kN/cm*^{2} and E_1*=3900kN/cm*^{2}, for the position of the force *P* at *g =L=200cm*. We see that as the cross section of the beam decreases, the forces H_1, H_2 and H_3 increase. An increase in the modulus of elasticity of concrete leads to an increase in H_1, a decrease in H_2 and a slight increase in H_3, followed by a steeper decrease with increasing crack size.

Example I- the modulus of elasticity of the concrete is $E_1 = 1700\left[kN/cm^2\right]$	*Example II*- the modulus of elasticity of the concrete is $E_1 = 3900\left[kN/cm^2\right]$
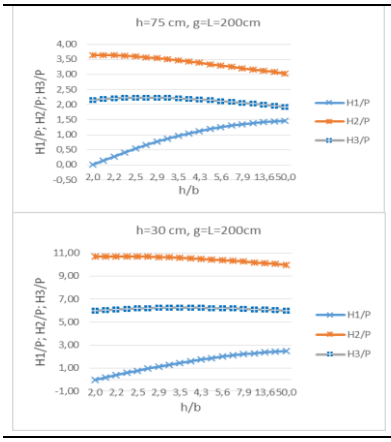	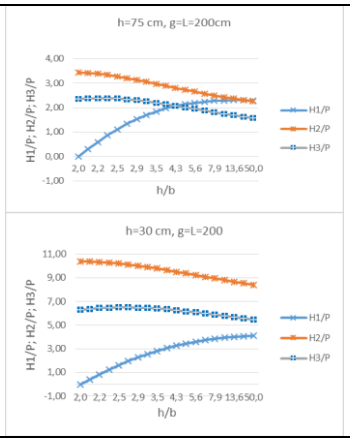
a)	b)

Figure 6. The parameters of the three support reactions for symmetrical cross section; a) *75/75cm* and *30/30cm* for E_1*=1700kN/cm*^{2}; b) *75/75cm* and *30/30cm* for E_1*=3900kN/cm*^{2}

Example I- the modulus of elasticity of the concrete is $E_1 = 1700\left[kN/cm^2\right]$	*Example II*- the modulus of elasticity of the concrete is $E_1 = 3900\left[kN/cm^2\right]$
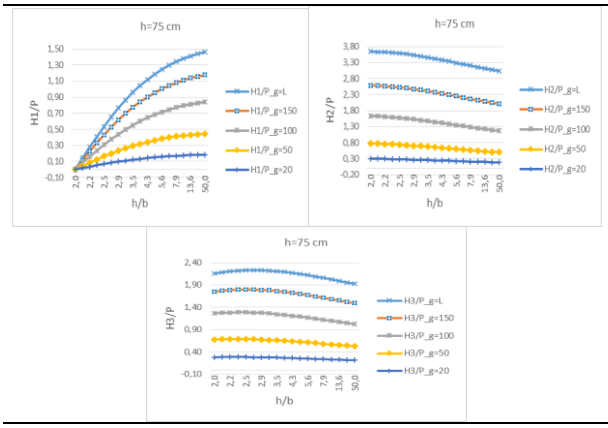	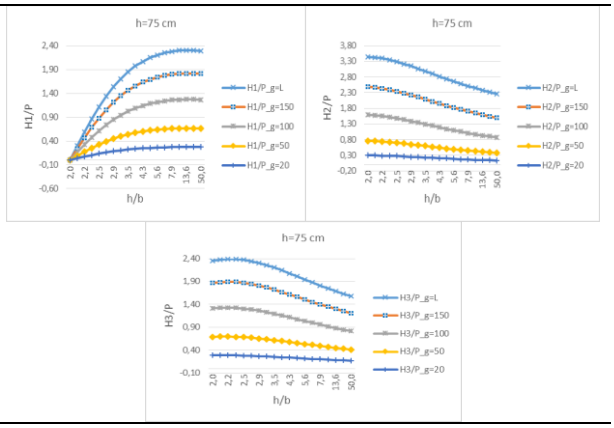
a)	b)
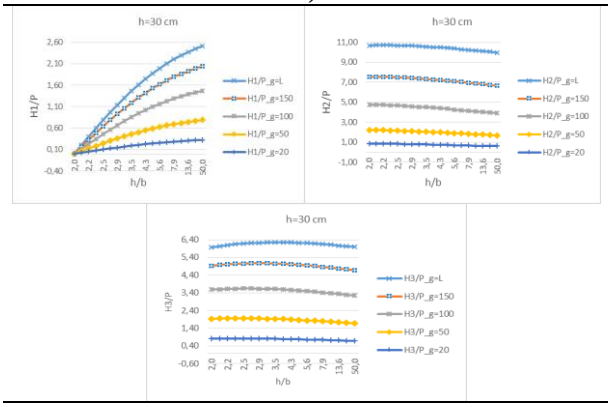	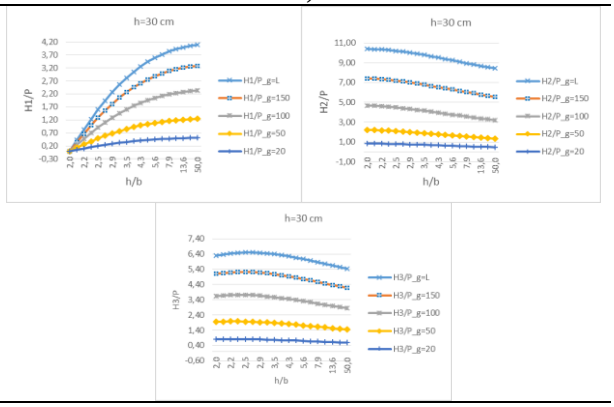
c)	d)

Figure 7. Changing the parameters of the three support reactions for values of *g=L=200cm; 150cm; 100cm; 50cm; 20cm* for various cross sections and E_1 modules; a) *75/75cm* E_1*=1700kN/cm*^{2}; b) *75/75cm* E_1*=3900kN/cm*^{2}; c) *30/30cm* E_1*=1700kN/cm*^{2}; d) *30/30cm* E_1*=3900kN/cm*^{2}

Figure 7 is a summary of the values to the parameters of the three support reactions for different positions of the force *P*, set by *g=L=200cm; 150cm; 100cm; 50cm; 20 cm*. We have two cross-sections, at two modulus of elasticity of concrete. From Figure 7 the same conclusions can be drawn as than Figure 6. H_1 has a value of 0 before the crack appears.

Case II – Asymmetrical Cross Section

The distance $b\left[cm\right]$ varies in the interval $\left[z_C, 0\right)$. It is monitored by the ratio h/b.

Example III- the modulus of elasticity of the concrete is $E_1 = 1700\left[kN/cm^2\right]$	*Example IV*- the modulus of elasticity of the concrete is $E_1 = 3900\left[kN/cm^2\right]$
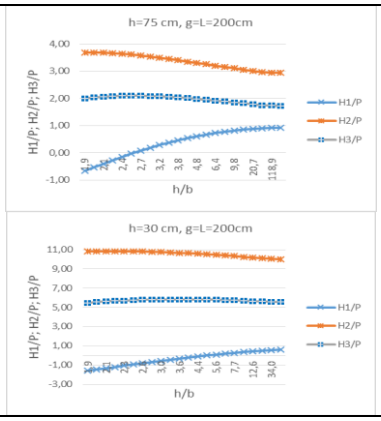	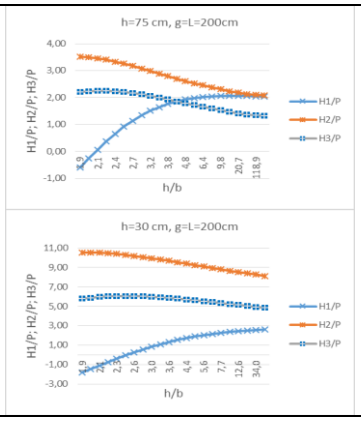
a)	b)

Figure 8. The parameters of the three support reactions for asymmetrical cross section; a) *75/75cm* and *30/30cm* for E_1=1700kN/cm^2; b) *75/75cm* and *30/30cm* for E_1=3900kN/cm^2

Example III- the modulus of elasticity of the concrete is $E_1 = 1700\left[kN/cm^2\right]$	*Example IV*- the modulus of elasticity of the concrete is $E_1 = 3900\left[kN/cm^2\right]$
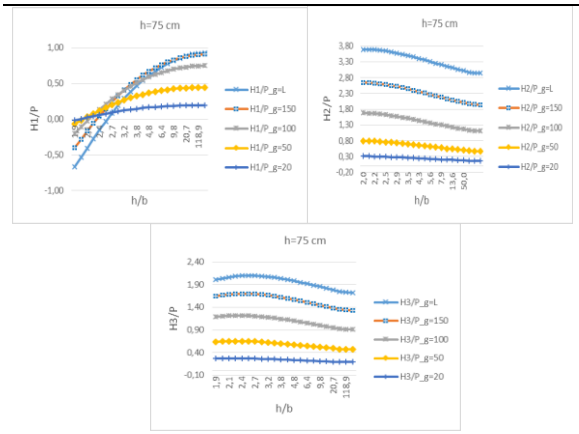	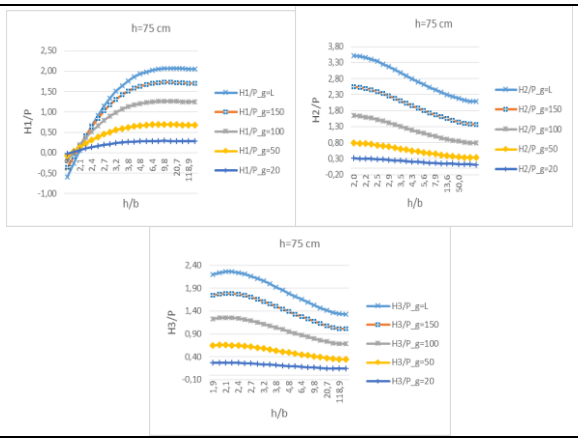
a)	b)
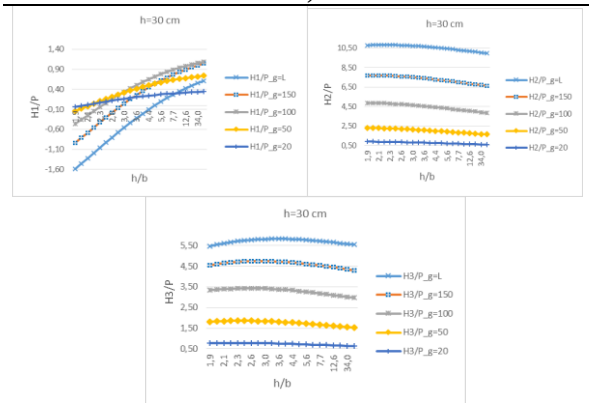	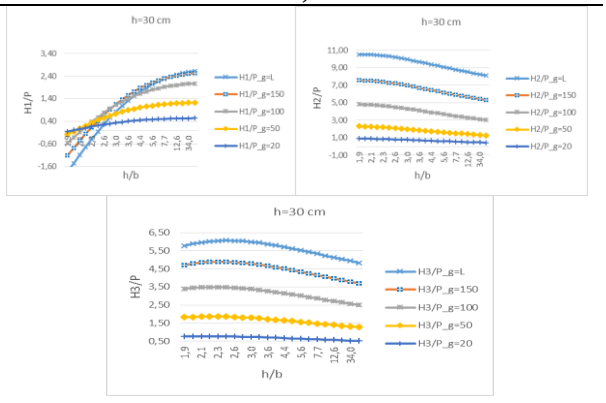
c)	d)

Figure 9. Changing the parameters of the three support reactions for values of *g=L=200cm; 150cm; 100cm; 50cm; 20cm* for various asymmetrical cross sections and E_1 modules; a) *75/75cm* E_1=1700kN/cm^2; b) *75/75cm* E_1=3900kN/cm^2; c) *30/30cm* E_1=1700kN/cm^2; d) *30/30cm* E_1=3900kN/cm^2

Figure 8 shows the parameters of the three support reactions for two asymmetric cross-sections - *75/75cm* and *30/30cm*, for two modulus of elasticity of concrete - E_1*=1700kN/cm*^{2} and E_1*=3900kN/cm*^{2}, for position of force *P* at *g=L=200cm*. The increasing trend of the three support reactions with decreasing cross-sectional size is maintained. It is noticeable that the increase in H_1 is weak. In the asymmetrical cross-sections, H_1 has negative values, until the appearance of a crack, i.e. it is on tension at the assumed cross-sectional shape. At E_1*=3900kN/cm*^{2} H_1 increases, H_2 decreases and H_3 slightly increases, and after *b/h= 2,4* it decreases steeply.

Figure 9 is a summary of the values of the parameters of the three support reactions for different positions of the force *P*, set by *g=L=200cm; 150cm; 100cm; 50cm; 20 cm*. We have two cross-sections, at two modulus of elasticity of concrete. The trend is maintained that as the cross section of the beam decreases, the forces increase. It is noteworthy that, while for all considered cases, moving the force *P* away from the support (*g* increases) leads to a rapid increase in H_1, for the smaller asymmetric cross-section – *30/30cm* H_1 has larger values at *g=150cm* and *100cm*. Increasing the modulus of elasticity of concrete results in an increase in H_1, a decrease in H_2, and a slight increase in H_3, followed by a steeper decrease with increasing crack size.

Case III - Symmetrical Cross Section Without Considering the Axial Force in the Potential Energy Expression

Example V- the modulus of elasticity of the concrete is $E_1 = 1700\left[kN/cm^2\right]$	*Example VI*- the modulus of elasticity of the concrete is $E_1 = 3900\left[kN/cm^2\right]$
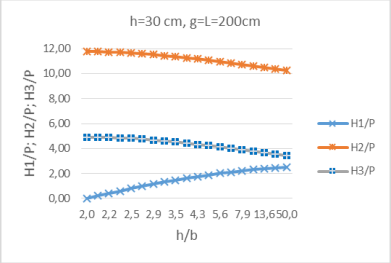	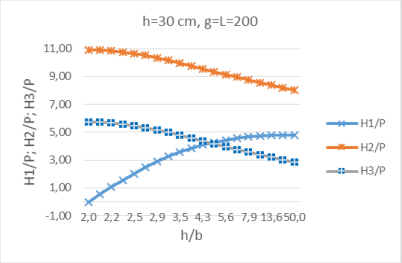
a)	b)

Figure 10. The parameters of the three support reactions for symmetrical cross section and neglected axial force; a) *30/30cm* for E_1*=1700kN/cm*^{2}; b) *30/30cm* for E_1*=3900kN/cm*^{2}

The comparison of Figure 6 and Figure 10 shows that neglecting the axial force in the strain potential energy expression does not lead to quantitative differences in H_1, while H_2 increases from *9%* to *2,5%*, H_3 decreases from *22%* to *75%* for E_1*= 1700kN/cm*^{2}. For E_1*=3900kN/cm*^{2}, H_1 increases from *20%* to *15%*, H_2 first increases from *5%* and then decreases to *4,6%*, H_3 decreases from *9%* to *90%*.

Example V - the modulus of elasticity of the concrete is $E_1 = 1700\left[kN/cm^2\right]$	*Example VI* - the modulus of elasticity of the concrete is $E_1 = 3900\left[kN/cm^2\right]$
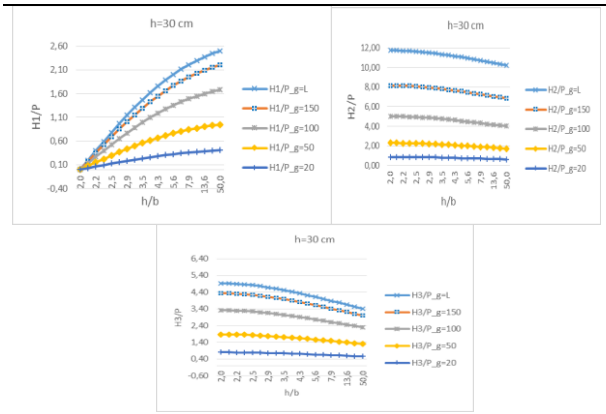	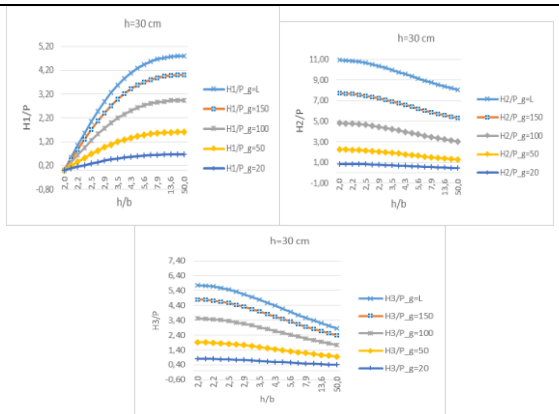
a)	b)

Figure 11. Changing the parameters of the three support reactions for values of *g=L=200cm; 150cm; 100cm; 50cm; 20cm* for various E_1 modules, symmetrical cross section and neglected axial force; a) *30/30cm* for E_1*=1700kN/cm*^{2}; b) *30/30cm* for E_1*=3900kN/cm*^{2}

A comparison of Figure 7 c) and d) with Figure 11 shows that H_1 is preserved without much change in value, H_2 increases, H_3 decreases for E_1=1700kN/cm^2. For E_1=3900kN/cm^2 H_1 increases, H_2 increases, H_3 decreases.

Case IV - Asymmetric Cross-Section Neglected Axial Force in the Strain Potential Energy Expression

Example VII- the modulus of elasticity of the concrete is $E_1 = 1700\left[kN/cm^2\right]$	*Example VIII*- the modulus of elasticity of the concrete is $E_1 = 3900\left[kN/cm^2\right]$
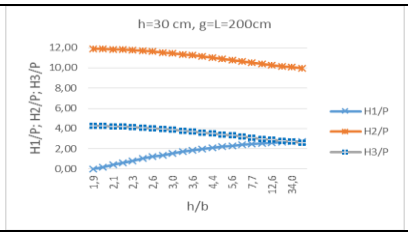	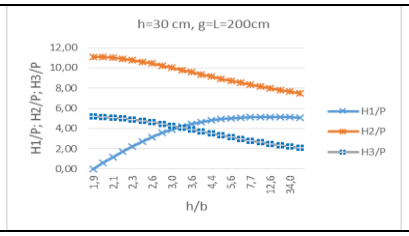
a)	b)

Figure 12. The parameters of the three support reactions for asymmetrical cross section and neglected axial force; a) *30/30cm* for E_1=1700kN/cm^2; b) *30/30cm* for E_1=3900kN/cm^2

A comparison of Figure 8 and Figure 12 shows that neglecting the axial force in the strain potential energy expression leads to an increase in H_1 about 2 times. H_2 remains almost unchanged, and H_3 decreases from *30%* to *110%*.

Example VII - the modulus of elasticity of the concrete is $E_1 = 1700\left[kN/cm^2\right]$	*Example VIII* - the modulus of elasticity of the concrete is $E_1 = 3900\left[kN/cm^2\right]$
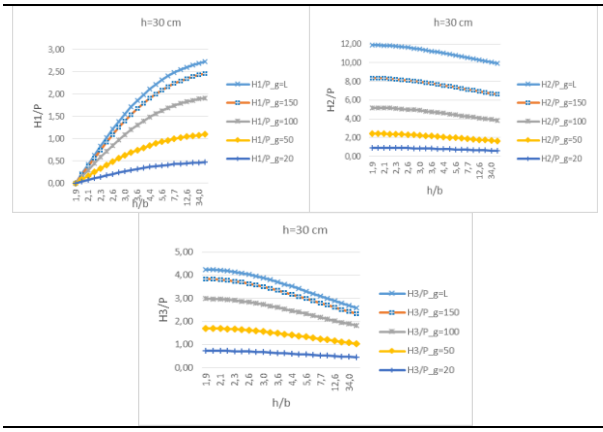	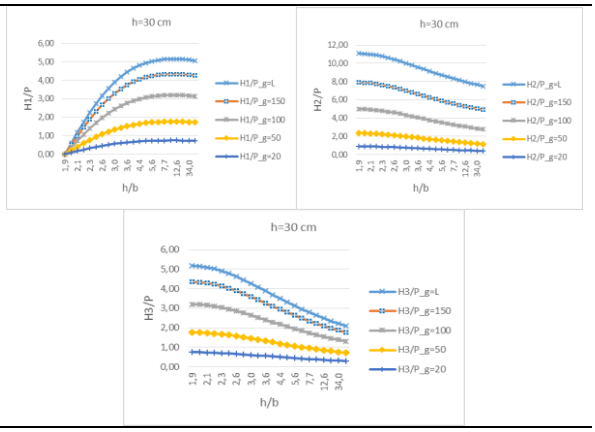
a)	b)

Figure 13. Changing the parameters of the three support reactions for values of *g=L=200cm; 150cm; 100cm; 50cm; 20cm* for various E_1 modules and asymmetrical cross section; a) *30/30cm* for E_1=1700kN/cm^2; b) *30/30cm* for E_1=3900kN/cm^2

Figure 13 shows the variation of the parameters of the three support reactions for an asymmetric cross-section of *30/30cm* for different positions of the loading force *P*, measured by the distance *g*. Values for two modulus of elasticity of concrete are demonstrated. It can be seen that as the concrete strength increases, H_1 increases, H_2 slightly decreases, and H_3 increases.

New Definition of Joint Shear in Interior RC Beam-Column Connection With the Calculated Forces H_1, H_2 and H_3.

We already know the magnitudes of the forces H_3; H_2' *and* H_1'. Then the determination of the Shear Force in RC Interior Beam-Column Connections instead of Eq. (3) will be by Eq. (40).

$$V_j = H_3 + H_2' + H_1' - V_c \tag{40}$$

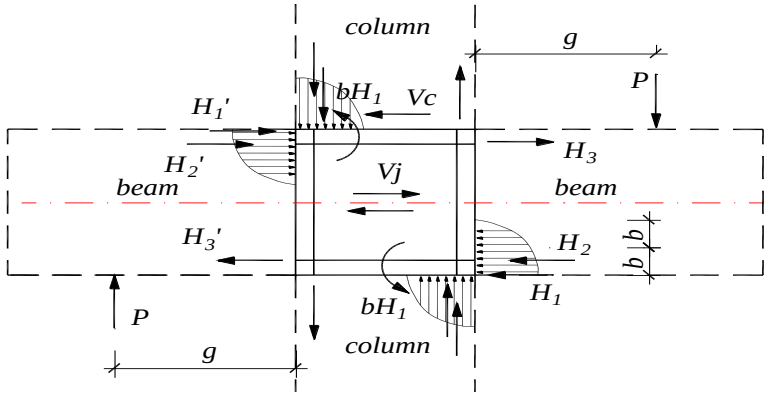

Figure 14. New definition of joint shear in interior RC beam-column connection with the calculated forces H_1, H_2 and H_3

If the frame is symmetric and other conditions being equal, we will have the equality of $H_1 = H_1'$, $H_2 = H_2'$ and $H_3 = H_3'$. Then Eq. (40) becomes Eq (41)

$$V_j = H_3 + H_2 + H_1 - V_c \,. \tag{41}$$

The comparison of Eq. (3) and Eq. (41) will be carried out by Eq. (42)

$$H_3 + H_2 + H_1 \overset{?}{=} \frac{M_b}{j_b} + \frac{M_b'}{j_b'} \,. \tag{42}$$

where - $M_b = Pg$ is the moment of the cantilever beam on the face of the column.

Comparison of the Results of Eq. (3) and Eq. (41) by Eq. (42)

Case I - symmetrical cross section

Example I- the modulus of elasticity of the concrete is $E_1 = 1700\left[kN/cm^2\right]$	*Example II*- the modulus of elasticity of the concrete is $E_1 = 3900\left[kN/cm^2\right]$
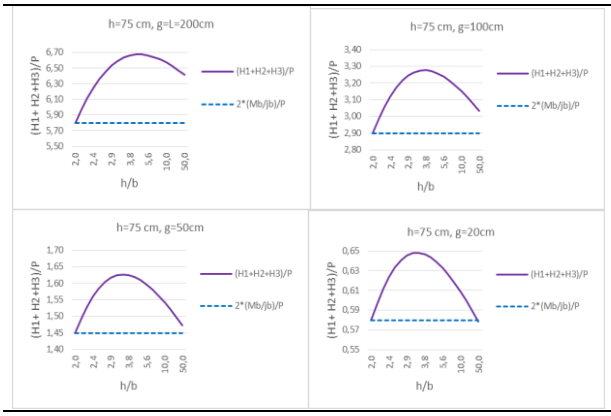	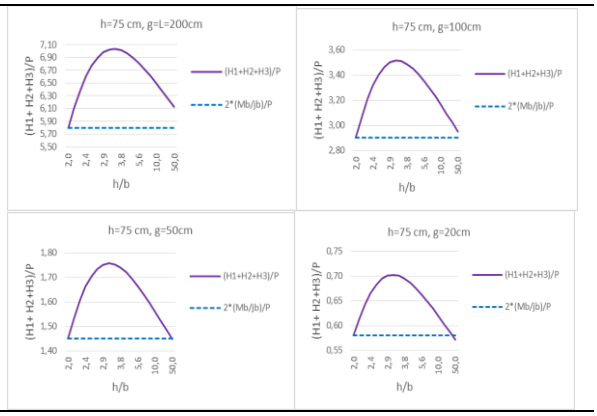
a)	b)

Figure 15. Comparison of the results of Eq. (3) and Eq. (41) for symmetrical cross section; a) *75/75cm* for E_1*=1700kN/cm*^{2}; b) *75/75cm* for E_1*=3900kN/cm*^{2}

Figure 15 shows comparison of the results of Eq. (3) and Eq. (41) for different possible positions of the force *P*, set by *g=L=200cm; g=100cm; g=50cm; g=20cm*. For all positions of the force *P*, the shear force determined with the exact values of the forces H_1, H_2 and H_3 is greater than what is recommended in the Eq. (3) - $\frac{M_b}{j_b} + \frac{M_b'}{j_b'}$. The difference is from *13.15%* to *10.57%*.

The following Table 1, Table2 and Table3 show the percentage differences between the part of the shear force determined according to Eq. (3) and the one calculated with the exact forces H_1, H_2 and H_3.

Table 1. Comparison of the results of Eq. (3) and Eq. (41) for symmetrical cross section

section		g	h/b	$\frac{H_3+H_2+H_1}{P}$	$\frac{\frac{M_b}{j_b}+\frac{M_b'}{j_b'}}{P}$	$\frac{(H_3+H_2+H_1)-\left(\frac{M_b}{j_b}+\frac{M_b'}{j_b'}\right)}{(H_3+H_2+H_1)}100\%$
Si me tri cal	75/75	200	4,3	6,67	5,80	13,15
		150	4,3	4,96	4,35	12,27
	E_1=1700	100	3,8	3,28	2,90	11,54
		50	3,5	1,63	1,45	10,92
		20	3,5	0,65	0,58	10,57
Si me tri cal	30/30	200	7,9	18,61	16,67	10,42
		150	4,8	13,68	12,5	8,61
	E_1=1700	100	3,8	8,98	8,33	7,22
		50	3,5	4,44	4,17	6,15
		20	3,2	1,77	1,67	5,61
Si me tri cal	75/75	200	3,5	7,04	5,80	17,61
		150	3,2	5,27	4,35	17,51
	E_1=3900	100	3,2	3,51	2,90	17,50
		50	3,2	1,76	1,45	17,49
		20	3,2	0,70	0,58	17,48
Si me tri cal	30/30	200	3,8	19,04	16,67	12,44
		150	3,5	14,13	12,5	11,52
	E_1=3900	100	3,5	9,34	8,33	10,76
		50	3,2	4,63	4,17	10,10
		20	3,2	1,85	1,67	9,74

Table 2. Comparison of the results of Eq. (3) and Eq. (41) for asymmetrical cross section

section		g	h/b	$\frac{H_3+H_2+H_1}{P}$	$\frac{\frac{M_b}{j_b}+\frac{M_b'}{j_b'}}{P}$	$\frac{(H_3+H_2+H_1)-\left(\frac{M_b}{j_b}+\frac{M_b'}{j_b'}\right)}{(H_3+H_2+H_1)}100\%$
Asi me tri cal	75/75	200	4,3	5,91	5,80	1,91
		150	3,8	4,54	4,35	4,14
	E_1=1700	100	3,5	3,10	2,90	6,46
		50	3,2	1,59	1,45	8,76
		20	3,2	0,65	0,58	10,14
Asi me tri cal	30/30	200	6,5	16,34	16,67	-2,02
		150	4,4	12,42	12,5	-0,64
	E_1=1700	100	3,6	8,44	8,33	1,23
		50	3,3	4,31	4,17	3,28
		20	3,0	1,75	1,67	4,55
Asi me tri cal	75/75	200	3,2	6,55	5,80	11,46
		150	3,2	5,02	4,35	13,37
	E_1=3900	100	2,9	3,42	2,90	15,25
		50	2,9	1,75	1,45	17,12
		20	2,9	0,71	0,58	18,20
Asi me tri cal	30/30	200	3,6	16,88	16,67	1,28
		150	3,3	12,94	12,5	3,41
	E_1=3900	100	3,0	8,83	8,33	5,58
		50	3,0	4,52	4,17	7,82
		20	3,0	1,83	1,67	9,11

The results of Table 1 show differences between the exact method ($H_3+H_2+H_1$) and the approximate method $\left(\frac{M_b}{j_b}+\frac{M_b'}{j_b'}\right)$ used in Eq.(3) for symmetrical section. For sections with normal concrete - E_1*=1700kN/cm*^{2} and large cross-sections (*75/75cm*) the differences between the two methods is more than *10%*, for all positions of the loading force *P (g=L=200cm; 150cm; 100cm; 50cm; 20cm).*For smaller cross-sections (*30/30cm*) the

difference is over *10%* only at *g=L=200cm*. When using high-strength concrete with $E_1=3900kN/cm^2$, all differences between the two methods, for all sections and all positions of the force, are over *10%*. For all types of concrete, the difference is greatest when the force *P* is farthest from the support.

The results in Table 2 are for an asymmetric cross-section. Close to *10%* are the differences between the two methods for the large cross-sections (*75/75cm*). When the concrete is high-strength, the differences increase and become greater than *10%* for the large cross-sections (*75/75cm*). The differences between the two methods are greatest for force *P* standing closer to the support.

Table 3. Comparison of the results of Eq. (3) and Eq. (41) for symmetrical cross section and without considering the axial force in the strain potential energy expression.

section		*g*	*h / b*	$\frac{H_3+H_2+H_1}{P}$	$\frac{\frac{M_b}{j_b}+\frac{M'_b}{j'_b}}{P}$	$\frac{(H_3+H_2+H_1)-\left(\frac{M_b}{j_b}+\frac{M'_b}{j'_b}\right)}{(H_3+H_2+H_1)}100\%$
Si me tri cal	30/30	200	3,2	17,37	16,67	4,03
		150	3,2	13,12	12,5	4,70
	E_1=1700	100	3,2	8,81	8,33	5,36
		50	3,2	4,43	4,17	6,01
		20	3,2	1,78	1,67	6,39
Si me tri cal	30/30	200	3,2	18,40	16,67	9,43
		150	3,2	13,95	12,5	10,39
	E_1=3900	100	3,2	9,40	8,33	11,32
		50	3,2	4,75	4,17	12,24
		20	3,2	1,91	1,67	12,78
Asi me tri cal	30/30	200	2,8	16,89	16,67	1,33
		150	2,8	12,88	12,5	2,91
	E_1=1700	100	2,8	8,72	8,33	4,45
		50	2,8	4,43	4,17	5,94
		20	2,8	1,79	1,67	6,81
Asi me tri cal	30/30	200	2,8	18,25	16,67	8,67
		150	2,8	13,94	12,5	10,30
	E_1=3900	100	2,8	9,46	8,33	11,87
		50	2,8	4,81	4,17	13,39
		20	2,8	1,94	1,67	14,27

The results of Table 3 show the differences between the exact method, (H_1+H_2+H_3) and the approximate one $\left(\frac{M_b}{j_b}+\frac{M'_b}{j'_b}\right)$ used in Eq. (3) for symmetric and asymmetric section *30/30cm*, when the contribution of the axial force in the expression of the potential energy of deformation is neglected. For ordinary concrete, the difference exceeds 5% when the force P is close to the support for both types of sections – symmetric and asymmetric. For both types of sections, with high-strength concrete, the differences exceed *10%*.

Conclusion

A solution of a cantilever beam with a special arrangement of the support devices and different possible positions of the loading force was carried out. The actual dimensions of the beam are taken into account. The influence of the material properties of its components are taken into account to.The obtained expressions for the reactions of the horizontal supports give results that clearly show the distribution of the forces along the height of the cantilever beam. Calculations were performed for a symmetric and asymmetric cross section. Results of varying only one material characteristic, the modulus of elasticity of the concrete, are shown. The support reactions of the cantilever beam for different positions of the loading force were calculated.

A comparison of the contribution of the cantilever beam forces to the shear force value for RC internal beam-column connections with that of the literature is made. The obtained results show differences in the amount of shear force determined in the two ways up to 18.20%. The complex nature of variation in the contribution of the

cantilever beam forces to the shear force value is demonstrated, given the multitude of monitored parameters and their influence on the results.

The obtained results represent an important part of the beam-column connection research in determining the force distributions with the variation of various parameters from the connected beams and columns. This article may be of interest to both researchers and practicing engineers in interpreting the results obtained from structural analyses.

Recommendations

This article will focused attention on how the forces are distributed from the cantilever beam along its height and the subsequent load from the beam on the beam-column connection with an emphasis on determining the shear force at the beam-to-column connection.

Scientific Ethics Declaration

The author declares that the scientific ethical and legal responsibility of this article published in EPSTEM journal belongs to the author.

Acknowledgements or Notes

* This article was presented as an oral presentation at the International Conference on Research in Engineering, Technology and Science (www.icrets.net) held in Thaskent/Uzbekistan on August 22-25, 2024.

References

Bakir, P. G., & Boduroglu, H. M. (2001). Re-evaluation of seismic capacity of interior beam-column joints. *WIT Transactions on The Built Environment*, *57*.

Celik, O. C., & Ellingwood, B. R. (2008). Modeling beam-column joints in fragility assessment of gravity load designed reinforced concrete frames. *Journal of Earthquake Engineering*, *12*(3), 357-381.

Doicheva, A. (2022). Off-center supported beam with additional elastic supports located at the height of the beam and asymmetrical cross section. In *International Conference on Basic Sciences, Engineering and Technology (ICBASET)* (pp. 120-129).

Doıcheva, A. (2023). Determination of the shear force in RC ınterior beam-column connections. *The Eurasia Proceedings of Science Technology Engineering and Mathematics*, *23*, 361-371.

Doicheva, A. (2023). Distribution of forces in RC ınterior beam–column connections. *Engineering Proceedings*, *56*(1), 114.

Doicheva, A.; Shu, Y.; Kusuhara, F. & Shiohara, H. (2023-3) Seismic tests on reinforced concrete beam-column joint sub-assemblages subject to lateral and long-term vertical load, *Structural Integrity and Life*, *23*(3), 269–276.

Gombosuren, D., & Maki, T. (2020). Prediction of joint shear deformation index of RC beam–column joints. *Buildings*, *10*(10), 176.

Hanson, N. W., & Connor, H. W. (1967). Seismic resistance of reinforced concrete beam-column joints. *Journal of the Structural Division*, *93*(5), 533-560.

Lowes L. & Altoontash A. (2003) Modeling reinforced-concrete beam-column joints subjected to cyclic loading. *Journal Structural Engineering*, 129, 1686–97.

Matlab R2017b, *The MathWorks Inc*., Natick, USA.

Park, R. & Paulay, T.,(1975), Reinforced concrete structuers, *John Wiley & Sons*

Paulay, T. (1989). Equilibrium criteria for reinforced concrete beam-column joints. *Structural Journal*, *86*(6), 635-643.

Shiohara, H. (2001) New model for shear failure of RC interior beam-column connection. *Journal of Structural Engineering*, *127*(2), 152-160

Tran, T. M., Hadi, M. N. S. & Pham, T. M. (2014). A new empirical model for shear strength of reinforced concrete beam – column connections. *Magazine of Concrete Research*, *66*(10), 514-530.

Uma, S. R., & Jain, S. K. (2006). Seismic design of beam-column joints in RC moment resisting frames-Review of codes. *Structural Engineering and Mechanics*, *23*(5), 579.

Yuan, F., Pan, J., Xu, Z., & Leung, C. K. Y. (2013). A comparison of engineered cementitious composites versus normal concrete in beam-column joints under reversed cyclic loading. *Materials and Structures*, *46*, 145-159.

Author Information

Albena Doicheva
University of Architecture, Civil Engineering and Geodesy (UACEG), Sofia 1164, 1 Hristo Smirnenski Blvd, Bulgaria,
Contact e-mail: *doicheva_fhe@uacg.bg*

To cite this article:

Doicheva, A. (2024). Shear force in RC internal beam-column connections for a beam loaded with a transverse force occupying different possible positions. *The Eurasia Proceedings of Science, Technology, Engineering & Mathematics (EPSTEM), 29,* 128-144.